frontiers in Materials

ORIGINAL RESEARCH
published: 18 October 2019
doi: 10.3389/fmats.2019.00256

Microwave Dielectric Properties of (1-x) Li_2MoO_4–xMg_2SiO_4 Composite Ceramics Fabricated by Cold Sintering Process

Yuping Ji[1], Kaixin Song[1], Xinjiang Luo[1], Bing Liu[1], Hadi Barzegar Bafrooei[1,2] and Dawei Wang[3]**

[1] Department of Electronics and Science and Technology, College of Electronic Information, Hangzhou Dianzi University, Hangzhou, China, [2] Department of Materials Science and Engineering, School of Engineering, Meybod University, Yazd, Iran, [3] Department of Materials Science and Engineering, The University of Sheffield, Sheffield, United Kingdom

Cold sintering process was successfully employed to fabricate (1-x) Li_2MoO_4–xMg_2SiO_4 (LMO-xMSO) microwave dielectric ceramics for 5G enabled technology. Dense LMO-xMSO ceramics were obtained with a high relative density in the range of 85–100% under the conditions of 200°C and 500 MPa in an hour. X-ray diffraction (XRD), scanning electron microscopy (SEM), energy dispersive X-ray spectroscopy (EDS), and Raman spectroscopy showed that both the LMO and MSO phases co-exist in all composite ceramics, and that there is no detectable secondary phase. Composites of LMO-xMSO ($0 < x < 0.3$) resonated at microwave frequency (∼9 GHz) with a low relative permittivity (ε_r) of 5.05∼5.3, and a high microwave quality factor (Q × f) of 9,450∼24,320 GHz, which are attractive for the applications of 5G enabled components.

Keywords: cold sintering, dielectric, composite ceramics, 5G, microwave properties

OPEN ACCESS

Edited by:
Di Zhou,
Xi'an Jiaotong University, China

Reviewed by:
Chunchun Li,
Guilin University of Technology, China
Wen Lei,
Huazhong University of Science and Technology, China

***Correspondence:**
Kaixin Song
kxsong@hdu.edu.cn
Dawei Wang
dawei.wang@sheffield.ac.uk

Specialty section:
This article was submitted to Functional Ceramics, a section of the journal Frontiers in Materials

Received: *28 August 2019*
Accepted: *25 September 2019*
Published: *18 October 2019*

Citation:
Ji Y, Song K, Luo X, Liu B, Barzegar Bafrooei H and Wang D (2019) Microwave Dielectric Properties of (1-x) Li_2MoO_4–xMg_2SiO_4 Composite Ceramics Fabricated by Cold Sintering Process. Front. Mater. 6:256. doi: 10.3389/fmats.2019.00256

INTRODUCTION

Microwave (MW) dielectric ceramics are a type of multifunctional material widely used for many basic components in communication systems, such as dielectric antenna, oscillators, substrates, and phase shifters (Cava, 2001; Reaney and Iddles, 2006; Zhou et al., 2018). With the rapid development of the fifth generation mobile cellular network (5G) and the requirements of new MW devices, it is necessary to explore novel dielectric materials in order to have fast signal response performance (Fiedziuszko et al., 2002; Ohsato, 2012; Sebastian et al., 2015; Faouri et al., 2019). MW ceramics with low permittivity (ε_r) and low energy loss are extensively used with microwave and millimeterwave (30–300 GHz) radio frequencies as circuit substrates and other functional dielectrics, due to their low signal transmission time delay (Sebastian, 2008). It is well-known that most MW ceramics are prepared by using high temperature solid-state sintering at temperatures greater than 1,200°C. Recently, the fabrication of microwave devices using low-temperature and ultra-low-temperature co-fired ceramic (LTCC and ULTCC) technology has attracted attention because it can make microwave ceramics compatible with sustainable and inexpensive electrodes, such as Ag, Cu, and Al, and meet the requirements of miniaturization, reliability, and low loss of microwave devices. However, there are still lots of problems between LTCC/ULTCC and electrodes, including the formation of parasitic phases by reaction, interdiffusion, and delamination, which is mainly due to their differences in thermal stability, shrinkage rates, and chemical incompatibilities (Green et al., 2008).

Cold sintering process (CSP) has recently been proposed as a method to produce different kinds of dense ceramics and composites under the condition of uniaxial pressure-assisted sintering (100–500 MPa) with low temperatures (<300°C) and short time periods (≤1 h), via utilizing water as a transient solvent (Kahari et al., 2014; Kähäri et al., 2016; Guo et al., 2016a,b, 2017; Induja and Sebastian, 2017; Randall et al., 2017; Väätäjä et al., 2017, 2018; Wang et al., 2018, 2019b). Kahari et al. directly pressed Li_2MoO_4 powder at room temperature with an appropriate amount of deionized water. The relative density and microwave dielectric properties of the cold-sintered sample was the same as that of a sample sintered at 540°C (Saraiva et al., 2017). Similarly, other molybdate ceramics such as $K_2Mo_2O_7$ (Guo et al., 2017), $(Bi_{0.95}Li_{0.05})(V_{0.9}Mo_{0.1})O_4$-$Na_2Mo_2O_7$ (Wang et al., 2019a), $(LiBi)_{0.5}MoO_4$ (Guo et al., 2017) etc. have been prepared by CSP with acceptable MW dielectric properties and a dense microstructure. Other than the low temperature, the key processing advantages of CSP are that it produces a near shape, that the prepared dense ceramic possesses the same diameter as the model, and that no reaction occurs between different ingredients. Randall et al. reported the fabrication and electrochemical properties of ceramic–salt composite electrolytes from cold sintering (Lee et al., 2019). Reaney et al. addressed cold sintered C0G mulitlayer ceramic capacitors with Ag internal electrodes (Wang et al., 2019b).

On the other hand, silicate ceramics are widely investigated as important low dielectric constant microwave and millimeterwave dielectrics. Pure Mg_2SiO_4 was reported to have a low permittivity (ε_r) of 6.8 and a high Q × f of 240,000 GHz (Tsunooka et al., 2003). Lai et al. reported a good temperature stability and a high Q × f of 237,400 GHz for low temperature (850–950°C) fired Mg_2SiO_4-Li_2TiO_3 composite ceramics (Lai et al., 2017). Zhang et al. reported that a high Q × f of 99,800 GHz for forsterite $(Mg_{1-x}Ni_x)_2SiO_4$ ceramics at a middle sintering temperature of 1,150°C (Zhang et al., 2014). To our knowledge, there are no reports on cold-sintered silicate ceramics or composites, which might exhibit promising features for 5G enabled technology.

In this work, Li_2MoO_4 and Mg_2SiO_4 were selected to fabricate (1-x) Li_2MoO_4–xMg_2SiO_4 composite ceramics (LMO-xMSO, x = 0, 5, 10, 15, 20, 30, 50, and 90 wt%) by CSP to show the possibility of fabricating dense silicate composite ceramics at a low temperature (≤200°C). The effects of MSO concentration on the microstructure and vibrational lattice modes, as well as microwave dielectric properties, were systematically discussed.

EXPERIMENTAL SECTION

MSO ceramic powders were prepared via a conventional solid-state sintering method using high purity powders MgO (Acros Organics, 99.99%) and SiO_2 (Acros Organics, 99.99%) as raw materials. Raw materials were weighed according to the nominal stoichiometric compositions, mixed with isopropanol, and ball-milled for 4 h in a planetary ball mill. Then the mixture was dried and calcined at 1,250°C for 4 h in air to synthesize the MSO samples. To prepare LMO-xMSO (x = 5, 10, 20, 30, 50, and 90 wt%) composite ceramics, the prepared MSO and commercially available LMO (Alfa Aesar, 99+%) powders were weighed by weight ratio and mixed with 10–15 wt% deionized water. The wet powders were uniaxially heated at 200°C for 60 min at a pressure of 500 Mpa. The pressed samples were dried in an oven at 120°C for 24 h.

The bulk densities of ceramic pellets were calculated by the geometric method. The room temperature phase combinations were identified by XRD (D2 Phaser, Bruker) using CuKα radiation. The Raman spectroscopy at room temperature was obtained using an in_Via Raman microscope with a green 514.5 nm laser (Renishaw). The microstructures of LMO-xMSO composite ceramics were characterized by a scanning electron microscope (SEM, Inspect F50, FEI) equipped with an energy dispersive spectrometer (EDS). The ε_r and Q × f value were identified by the $TE_{01\delta}$ dielectric resonator method using a R3767CH, Advantest Corporation (Tokyo, Japan) vector network analyzer.

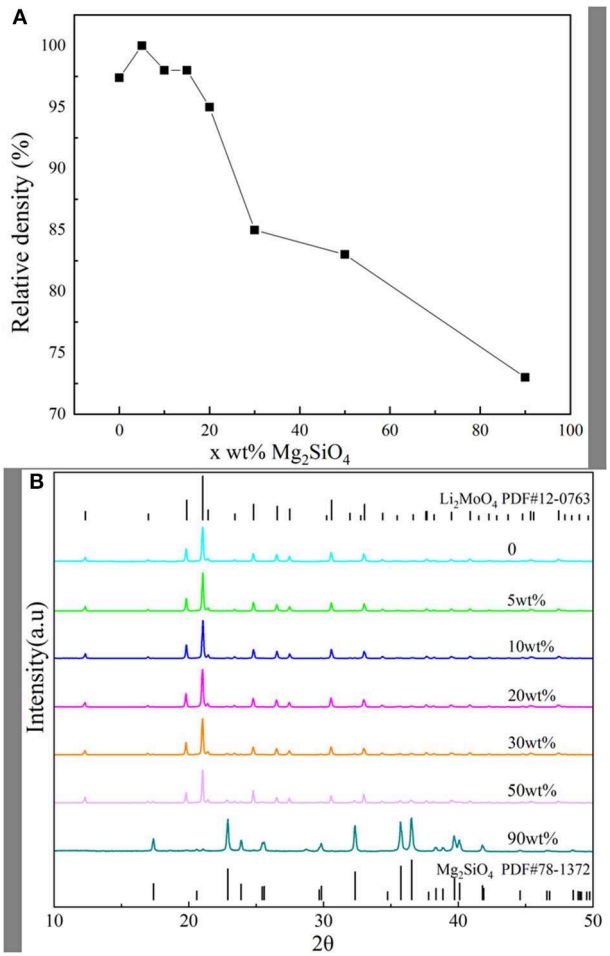

FIGURE 1 | (A) Relative densities and **(B)** XRD patterns of (1-x) LMO-xMSO composite ceramics.

RESULTS AND DISCUSSION

Figure 1A presents the relative density (ρr) of LMO-xMSO composite ceramic samples. A high relative density of 85–100% was obtained in LMO-xMSO composite ceramics with $x < 50\%$, which fully demonstrates that dense LMO-xMSO samples can be produced by cold-sintering with the assistance of deionized water where LMO is predominant. **Figure 1B** shows the XRD patterns at room temperature of LMO-xMSO composite samples with 2θ of 10°-50°. MSO has an island structure (space group Pbnm, JCPDS No.78#1372). LMO has a triangular structure (space group R3, JCPDS No.12#0763) with tetrahedral coordination that was formed by a separate MoO_4 tetrahedron (Barinova et al., 2014; Saraiva et al., 2017). It is clear that two sets of diffraction

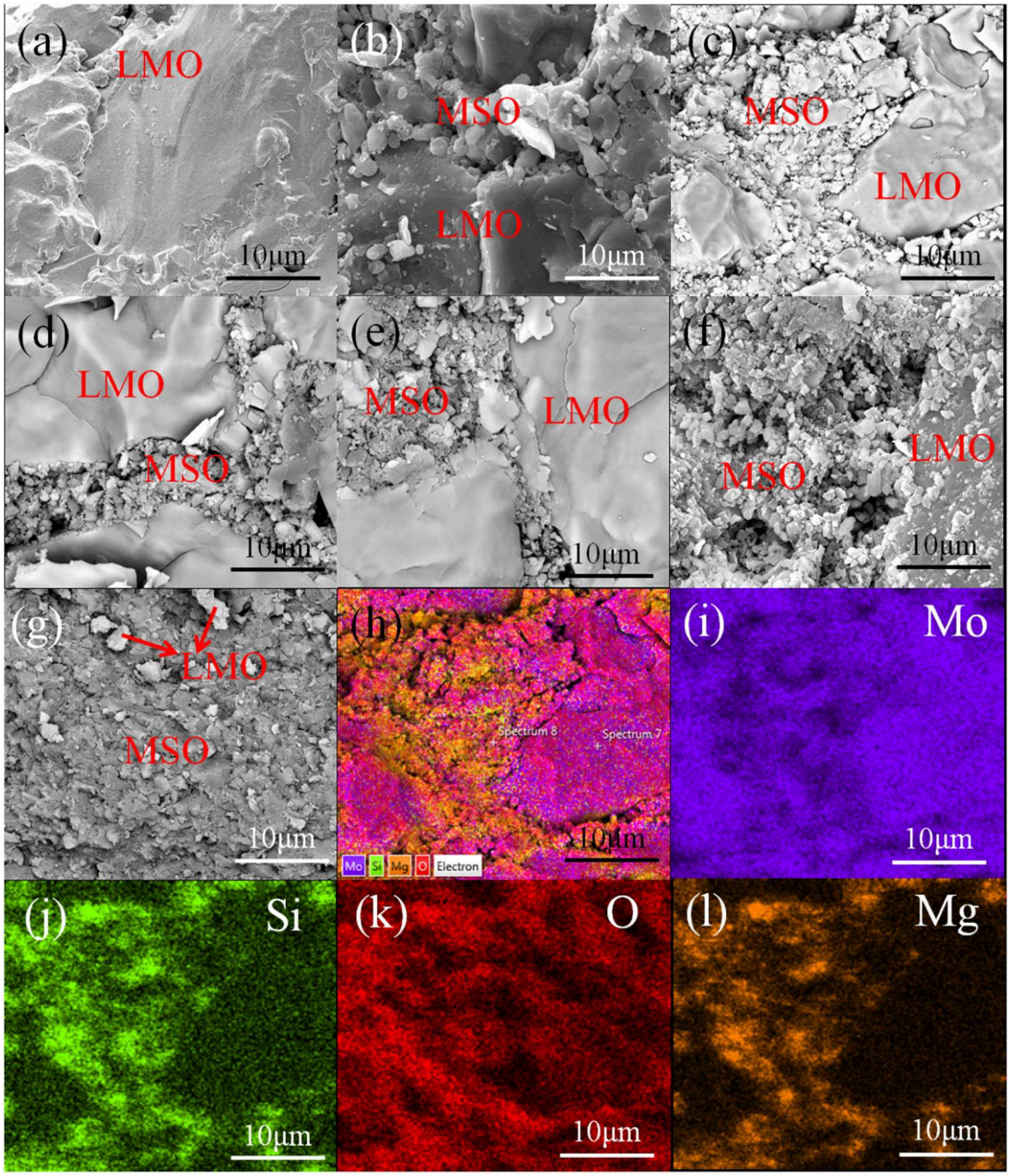

FIGURE 2 | SEM images of cold-sintered **(a)** LMO; **(b)** 95 wt% LMO−5 wt% MSO; **(c)** 90 wt% LMO−10 wt% MSO; **(d)** 80 wt% LMO−20 wt% MSO; **(e)** 70 wt% LMO−30 wt% MSO; **(f)** 50 wt% LMO−50 wt% MSO and **(g)** 10 wt% LMO−90 wt% MSO composite ceramics; EDS element mapping of LMO-MSO: **(h)** element layered image; **(i)** Mo; **(j)** Si; **(k)** O and **(l)** Mg.

peaks co-exist without impurities found, corresponding to LMO and MSO phases, respectively, indicating that there are no chemical reactions happening between MSO and LMO.

SEM images of cold-sintered LMO-xMSO composite ceramics are given in **Figures 2a–g**. The SEM images reveal dense microstructures. It can be clearly observed that there are two discrete phases present in all composite ceramic samples, with the smaller MSO grains surrounding larger LMO grains, in agreement with the X-ray results (**Figure 1B**). According to the morphology feature and EDS analysis (**Figures 2h-l**), the large and small grains are LMO and MSO grains, respectively.

Figure 3 shows the Raman spectra of LMO-xMSO composites at room-temperature ranging from 50 to 1,200 cm^{-1}. According to group theory and irreducible representations, LMO and MSO have 82 and 84 different vibration modes, respectively, as described below:

$$\Gamma_{LMO} = 21A_g + 20A_u + 21E_g + 20E_u \quad (1)$$

$$\Gamma_{MSO} = 11A_g + 25B_g + 10A_u + 38B_u \quad (2)$$

For both LMO and MSO, the corresponding Raman active modes are described as 42 ($21A_g + 21E_g$) and 36 ($11A_g + 25B_g$), respectively. The E_u and B_u of LMO and MSO are infrared active. Generally, vibrations can be divided into internal and external modes (Barinova et al., 2014; Saraiva et al., 2017). For LMO, the vibrations of the MoO_4 tetrahedron trigger the internal modes, and the movement of Li^+ cations and the vibrational/translations of the $[MoO_4]$ tetrahedron are related to the external modes (Porto and Scott, 1967; Guo et al., 2014). The Raman bands of LMO are roughly divided into three parts: the bands below 85 cm^{-1} are due to the translational motions of external modes, most of the bands between 85 and 800 cm^{-1} belong to a mixture of external and internal modes, and the bands above 800 cm^{-1} are assigned to the stretching (ν_1 and ν_3) of internal modes. MSO has the crystal structure of forsterite, the binding force of Si-O bonds between atoms inside the silicon tetrahedron is stronger than that between Mg and silicon tetrahedron, and the two strongest Raman bands 824.6 cm^{-1} and 856.7 cm^{-1} are assigned to the symmetrical stretching vibration modes (ν_1) of the silicon tetrahedron and the antisymmetric stretching vibration modes (ν_3). The bands above 800 cm^{-1} are related to the S (Si-O) stretching modes. 400–700 cm^{-1} is dominated by the Si-O vibration modes. According to the internal modes and the external modes, the bands above 430 cm^{-1} are assigned to the stretching motions (ν_1 and ν_3) and the bending motions (ν_2 and ν_4) of the internal modes. The bands below 430 cm^{-1} are related to external modes and are divided into rotational modes (B_g close to 370 cm^{-1}) and translational modes. As the amount of MSO content decreases, the strength of LMO Raman bands peak increases gradually, and the Raman bands of LMO (Ag $\sim$ 68 cm^{-1}, $\nu_1 \sim$ 819 cm^{-1} and ν_1 / $\nu_3 \sim$ 902 cm^{-1}) are distinctly diaplayed in all LMO-xMSO composites. The Raman spectra of LMO-xMSO composite ceramics are composed of a superposition of the spectral characteristics of LMO and MSO phases, and the coexistence of LMO and MSO in composites is further confirmed.

The relative permittivity (ε_r) and quality factor (Q×f value) of LMO-xMSO composite ceramics with different MSO weight fractions and a series comparative experimental date are listed in **Table 1**. It can be seen from **Table 1** that cold-sintered pure LMO ceramics at 120°C, 400 MPa for 30 min, exhibit a relative density of 97.4%, $\varepsilon_r \sim 5.3$, and Q×f $\sim$ 24,320 GHz, which is equivalent to those fabricated by the conventional sintering method. As the MSO fraction increases, both ε_r and Q×f are found to decrease from 5.3 and 24,320 to 5.05 and 9,450 GHz, respectively. The τ_f value of LMO-xMSO is in the range of −161 to −118, and does not greatly improve the τ_f compared to LMO.

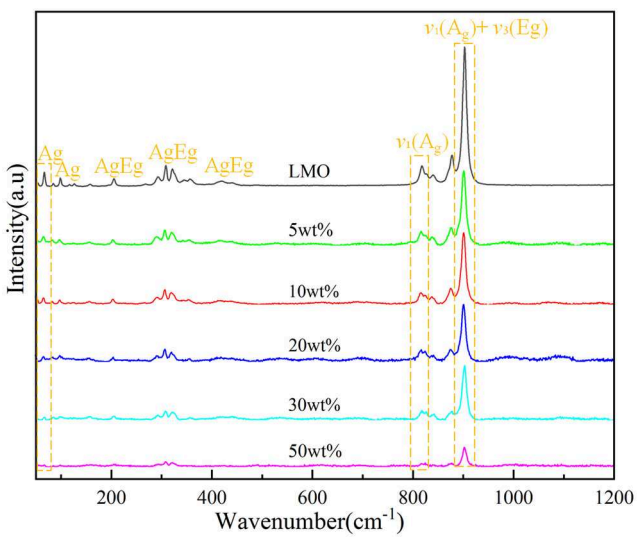

FIGURE 3 | Raman spectra of (1-x) LMO-xMSO composite ceramics.

CONCLUSIONS

In this work, novel LMO-xMSO microwave composite ceramics with high relative densities of > 80% were successfully prepared by CSP (200°C, 60 min, and 500 MPa). Two characteristic phases of LMO and MSO were found in all composite ceramics. The

TABLE 1 | Sintering temperatures, densities, and microwave dielectric properties of LMO-xMSO composite ceramics.

Composition	ST [C]	ρ_r (%)	ε_r	Q × f (GHz)
LMO	120	97.4	5.3	24,320
5 wt%MSO	200	100	5.15	22,270
10 wt%MSO	200	98	5.1	19,430
15 wt%MSO	200	98	5.1	18,530
20 wt%MSO	200	90	5.05	16,030
30 wt%MSO	200	85	5.07	9,450
LMO	540	95.5	5.5	46,000

result of XRD, SEM, and Raman spectroscopy indicated that there was no chemical reaction between the two phases. With the increase of the MSO weight fraction ε_r decreased from 5.3 to 5.05, and the Q×f value decreased from 24,320 to 9,450 GHz. The successful preparation of (1-x) LMO-xMSO composite ceramics indicates that CSP has great potential in the low temperature fabrication of microwave composite ceramics for 5G enabled technology.

DATA AVAILABILITY STATEMENT

All datasets generated for this study are included in the manuscript/supplementary files.

AUTHOR CONTRIBUTIONS

All authors listed have made a substantial, direct and intellectual contribution to the work, and approved it for publication.

FUNDING

This work was supported by the National Natural Science Foundation of China under grant number 51672063 and 51802062, and Open projects of Key Laboratory of inorganic functional materials and devices, Shanghai silicate institutes (KLIFMD201708).

REFERENCES

Barinova, O., Kirsanova, S., Sadovskiy, A., and Avetissov, I. (2014). Properties of Li_2MoO_4 single crystals grown by Czochralski technique. *J. Cryst. Growth* 401, 853–856. doi: 10.1016/j.jcrysgro.2013.10.051

Cava, R. J. (2001). Dielectric materials for applications in microwave communications. *J. Mater. Chem.* 11, 54–62. doi: 10.1039/b003681l

Faouri, S. S., Mostaed, A., Dean, J. S., Wang, D., Sinclair, D. C., Zhang, S., et al. (2019). High quality factor cold sintered Li_2MoO_4-$BaFe_{12}O_{19}$ composites for microwave applications. *Acta Mater.* 166, 202–207. doi: 10.1016/j.actamat.2018.12.057

Fiedziuszko, S. J., Hunter, I. C., Itoh, T., Kobayashi, Y., Nishikawa, T., Stitzer, S. N., et al. (2002). Dielectric materials, devices, and circuits. *IEEE Trans. Microw. Theor. Tech.* 50, 706–720 doi: 10.1109/22.989956

Green, D., J., Guillon, O., and Rçdel, J. (2008). Constrained sintering: a delicate balance of scales. *J. Eur. Ceram. Soc.* 28, 1451–1466. doi: 10.1016/j.jeurceramsoc.2007.12.012

Guo, J., Baker, A. L., Guo, H., Lanagan, M. T., and Randall, C. A. (2017). Cold sintering process: a new era for ceramic packaging and microwave device development. *J. Am. Ceram. Soc.* 100, 669–677. doi: 10.1111/jace.14603

Guo, J., Berbano, S. S., Guo, H., Baker, A. L., Lanagan, M. T., and Randall, C. A. (2016a). Cold sintering process of composites: bridging the processing temperature gap of ceramic and polymer materials. *Adv. Funct. Mater.* 26, 7115–7121. doi: 10.1002/adfm.201602489

Guo, J., Guo, H., Baker, A. L., Lanagan, M. T., Kupp, E. R., Messing, G. L., et al. (2016b). A Cold sintering: a paradigm shift for processing and integration of ceramics. *Angew. Chem. Int. Ed.* 55, 11457–11461. doi: 10.1002/anie.201605443

Guo, J., Zhou, D., Li, Y., Shao, T., Qi, Z. M., Jin, B. B., et al. (2014). Structure-property relationships of novel microwave dielectric ceramics with low sintering temperatures: (Na0.5xBi0.5xCa1-x)MoO4. *Dalton Trans.* 43, 11888–11896. doi: 10.1039/C4DT00838C

Induja, I. J., and Sebastian, M. T. (2017). Microwave dielectric properties of mineral sillimanite obtained by conventional and cold sintering process. *J. Eur. Ceram. Soc.* 37, 2143–2147. doi: 10.1016/j.jeurceramsoc.2017.01.007

Kahari, H., Teirikangas, M., Juuti, J., and Jantunen, H. (2014). Dielectric properties of lithium molybdate ceramic fabricated at room temperature. *J. Am. Ceram. Soc.* 97, 3378–3379. doi: 10.1111/jace.13277

Kähäri, H., Teirikangas, M., Juuti, J., and Jantunen, H. (2016). Room-temperature fabrication of microwave dielectric Li_2MoO_4-TiO_2 composite ceramics. *Ceram. Int.* 42, 11442–11446. doi: 10.1016/j.ceramint.2016.04.081

Lai, Y., Hong, C., Jin, L., Tang, X., Zhang, H., Huang, X., et al. (2017). Temperature stability and high-Qf of low temperature firing Mg2SiO4–Li2TiO3 microwave dielectric ceramics. *Ceram. Int.* 43, 16167–16173. doi: 10.1016/j.ceramint.2017.08.192

Lee, W., Lyon, C. K., Seo, J.-H., Lopez-Hallman, R., Leng, Y., Wang, C.-Y., Hickner, M. A., et al. (2019). Ceramic–salt composite electrolytes from cold sintering. *Adv. Electron. Mater.* 29:1807872. doi: 10.1002/adfm.201807872

Ohsato, H. (2012). Functional advances of microwave dielectric for next generation. *Ceram. Int.* 38, S141–S146. doi: 10.1016/j.ceramint.2011.04.068

Porto, S. P. S., and Scott, J. F. (1967). Raman spectra of CaWo4, SrWO4, CaMoO4, and SrMoO4. *Phys. Rev.* 157, 716–719. doi: 10.1103/PhysRev.157.716

Randall, C. A., Guo, J., Guo, H., Baker, A., and Lanagan, M. T. U. S. (2017). *Cold Sintering Ceramics and Composites.* U.S. Provisional Patent Application No 20170088471. University Park, PA: The Penn State Research Foundation. Available online at: http://www.freepatentsonline.com/y2017/0088471.html

Reaney, I. M., and Iddles, D. (2006). Microwave dielectric ceramics for resonators and filters in mobile phone networks. *J. Am. Ceram. Soc.* 89, 2063–2072. doi: 10.1111/j.1551-2916.2006.01025.x

Saraiva, G. D., Paraguassu, W., Freire, P. T. C., Ramiro de Castro, A. J., de Sousa, F. F., and Mendes Filho, J. (2017). Temperature induced phase transformations on the Li_2MoO_4 system studied by Raman spectroscopy. *J. Mol. Struct.* 1139, 119–124. doi: 10.1016/j.molstruc.2017.03.038

Sebastian, M., T., and Ubic, R., Jantunen, H. (2015). Low-loss dielectric ceramic materials and their properties. *Int. Mater. Rev.* 60, 392–412. doi: 10.1179/1743280415Y.0000000007

Sebastian, M. T. (2008). *Dielectric Materials for Wireless Communication.* Oxford: Elsevier.

Tsunooka, T., Androu, M., Higashida, Y., and Sugiura, H. (2003). Effects of TiO_2, on sinterability and dielectric properties of high-Q forsterite ceramics. *J. Eur. Ceram. Soc.* 23, 2573–2578. doi: 10.1016/S0955-2219(03)00177-8

Väätäjä, M., Kähäri, H., Juuti, J., and Jantunen, H. (2017). Li_2MoO_4-based composite ceramics fabricated from temperature-and atmosphere-sensitive MnZn ferrite at room temperature. *J. Am. Ceram. Soc.* 100, 3626–3635. doi: 10.1111/jace.14914

Väätäjä, M., Kähäri, H., Ohenoja, K., Sobocinski, M., Juuti, J., and Jantunen, H. (2018). 3D printed dielectric ceramic without a sintering stage. *Sci. Rep.* 8:15955. doi: 10.1038/s41598-018-34408-5

Wang, D., Zhang, S., Zhou, D., Song, K., Feteira, A., Vardaxoglou, Y., et al. (2019a). Temperature stable cold sintered $(Bi_{0.95}Li_{0.05})(V_{0.9}Mo_{0.1})O_4$-$Na_2Mo_2O_7$ microwave dielectric composites. *Materials* 12:1370. doi: 10.3390/ma12091370

Wang, D., Zhou, D., Song, K., Feteira, A., Randall, C. A., and Reaney, I. M. (2019b). Cold sintered C0G multilayer ceramic capacitors. *Adv. Electron. Mater.* 5:1900025. doi: 10.1002/aelm.201900025

Wang, D., Zhou, D., Zhang, S., Vardaxoglou, Y., Whittow, W. G., Cadman, D., et al. (2018). Cold-sintered temperature stable $Na_{0.5}Bi_{0.5}MoO_4$-Li_2MoO_4 microwave composite ceramics. *ACS Sustain. Chem. Eng.* 6, 2438–2444. doi: 10.1021/acssuschemeng.7b03889

Zhang, C., Zuo, R., Zhang, J., and Wang, Y. (2014). Structure-dependent microwave dielectric properties and middle-temperature sintering of forsterite $(Mg_{1-x}Ni_x)_2SiO_4$ ceramics. *J. Am. Ceram. Soc.* 98, 702–710. doi: 10.1111/jace.13347

Zhou, D., Pang, L., Wang, D., and Reaney, I. M. (2018). $BiVO_4$ based high k microwave dielectric materials: a review. *J. Mater. Chem. C.* 6, 9290–9313. doi: 10.1039/C8TC02260G

Conflict of Interest: The authors declare that the research was conducted in the absence of any commercial or financial relationships that could be construed as a potential conflict of interest.